Modelling of water droplets heat and mass transfer in the course of phase transitions. II: Peculiarities of the droplet radial coordinate and the time grid calibration

Gintautas Miliauskas, Arvydas Adomavičius, Monika Maziukienė

Department of Thermal and Nuclear Energy,
Kaunas University of Technology
Studentų str. 56, LT-51424 Kaunas
gimil@ktu.lt

Abstract. This paper continues optimization of numerical solution algorithm of iterative scheme grid for the *droplet* task, which was presented in the first article of this series. Assumptions were made by optimal assessable number of members, which was already defined in numerical experiment in case of compound heat spread by conduction and radiation, and an unsteady temperature field was described by infinite integral equation sum. For the convenience of numerical analysis, droplet thermal parameters P_T were described by universal Fourier criteria Fo and by dimensionless radial coordinate η function $P_T(\mathrm{Fo}, \eta)$. This function is given in form of infinite integral equation sum with each thermal parameter having a distinct initial member and individually defined subsidiary function. This function is given in form of infinite integral equation sum with each thermal parameter having a distinct initial member and individually defined subsidiary function. The droplet time and radial coordinate grading change influence for calculated function graphs $P_T(\mathrm{Fo}, \eta)$ was evaluated by water droplets heat transfer and phase transformation numerical experiment. Summarizing by conduction and radiation heated water droplets thermal parameter variation patterns, a methodology of forming an optimal grid for *droplet* task iterative solving is provided.

Keywords: water droplets, heat and mass transfer, Fourier time scale, phase transformation cycle, numerical scheme, optimal grid.

1 Introduction

Technologies based on liquid droplet transfer processes are attractive by the fact that, when spraying out the liquid, the contact surface between liquid and gaseous phases increases significantly. The latter, in heat and mass transfer processes, is one of the main factors determining their intensity. Therefore, the definition of transfer process intensity in various thermal technologies was and is in the field of stable researcher

attention [15]. This is confirmed by the statistics of publications on droplet problem issues; to the request of water droplet evaporation, the database [17] provides over forty-three thousand recognized ISI level scientific articles. The publication growth trend is noticeable (year/the number of articles): 2000/789; 2005/1219; 2010/1891; 2013/2857; 2014/2964; 2015/2314. In the droplet problem, near the dominating direction of water droplets heat and mass transfer research [2,4,11,14], a traditional of carbohydrate [3,5,17] and new biofuel droplet trends can be distinguished [13, 17].

The abundance of scientific articles concerning *droplet* issues makes a detailed their analysis unrealistic. Therefore, it is necessary to distinguish narrower *droplet* research directions and to define angular aspects of analysis. The historical *droplet* research development, as well as the applied method genesis, is characterized by a wide range of tasks, growing maturity, and deepening physical interpretation of researched transfer processes [1, 12, 15]. Assumptions for systemic *droplet* research evaluation are created by droplet phase transformation cycle that combines various sprayed liquid phase transformations regimes as well as defining of heat and mass transfer droplet parameters P grouping into thermal P_T energetic P_q, dynamic P_d and phase transition P_f groups [10]. For thermal technologies practice, it is important to define phase transformation rate in gas and liquid two-phase flow. Therefore, the liquid vapour flow on the surface of the droplet g_v considered to be one of the most important parameter P_f in liquid spray technologies. It is defined by totality of thermal, energetic, and dynamic parameters, which is conditioned by the compound transfer and phase transformation processes interaction that occur in the two phase flow. Therefore, in *droplet* research the complex evaluation becomes relevant for transformation process interaction. Its quality depends from assumptions that are made by the researcher. The researchers approach is important to the contact between phase surface temperatures role into droplet transformation process interaction. In regular sprayed liquid thermal technologies (burning of fuel in furnaces and engines, gas temperature regulation, air conditioning, utilization of heat from smoke and, so on), the contact surface temperature $T_{R,vg}$ between the liquid and gas phases can be equated to the droplet surface temperature $T_{R,vg} \cong T_R$. Evaporating droplet surface temperature is between the dew point T_{dp} and saturation temperatures T_s: $T_{dp} < T_R < T_s$. In the case of small micron row droplets, it is necessary to evaluate a possible temperature jump in the Knudsen layer ΔT_{Kn}, which surrounds the evaporating droplets: $T_{R,vg} \equiv T_R + \Delta T_{Kn}$ [9, 16]. This is very important in the nanotechnology level. Assumption $T_R \approx T_s$ is regarded as very rough.

In droplet phase transformation cycle, the contact surface temperature between liquid and gaseous is changing. This time τ change is described by function $T_R \equiv T_R(\tau)$ and can only be defined by coupled analysis of the heat flows within the droplet and its surroundings. It is necessary to define heat flow balance conditions that describes flows in and flows from the droplet surface.

The heat flows interaction on the droplet surface heated by conduction and radiation is described by mathematical *droplet* model that has been discussed in the first paper of this cycle [8]. It is based on unsteady temperature field in spherical semitransparent liquid droplet integral-type model of time τ and radial coordinate r functions $T(r, \tau)$ [6]. The function $T(r, \tau)$ is defined numerically when at the iterative cycle, a heat flow balance on

the droplet surface must be provided by requiring dependability to ensure a condition:

$$\vec{q}_{\Sigma}^{\,+} + \vec{q}_{\Sigma}^{\,-} + \vec{q}_{f}^{\,+} \equiv 0. \tag{1}$$

In expression (1), q is heat flow density, indices Σ and f shows a compound heat flows of transfer and phase transformation, respectively. Meanwhile, signs "$-$" and "$+$" define attribution of parameter for droplet surface internal and external sides, respectively.

It is justified by the numerical experiment [8] that it is optimal to evaluate about 120 members in the infinite integral equation series when describing the function $T(r, \tau)$. Then imbalance of calculated heat flows on a droplet surface is ensured by less than one hundredth percent. In this work, a problem of droplet thermal parameters is solved for the optimal grading of time and droplet radial coordinate in *droplet* task numerical solution at the iterative scheme.

2 A balance of heat flows on the surface of a droplet and droplet thermal parameters model

For the liquid spraying technologies, a variety of transfer processes conditions that is going on in two-phase gas and droplet flows is inherent. Functions $P(\tau)$ that describe the variation of sprayed liquid droplet heat and mass transfer parameters are distinctive in different technologies. Peculiarities of functions $P(\tau)$ are defined by the conditions of droplets heat and mass transfer in gas flow. Sprayed liquid and gas flow parameters influence is significant. The following parameters are also important: sprayed liquid temperature $T_{l,0}$, droplet initial radius that defines their dispersity R_0, droplets slipping velocity in gas Δw_l, gas mixture initial temperature $T_{g,0}$, by liquid vapour partial pressure $p_{v,\infty}$ and gas pressure p_g ratio expressed a liquid vapour volume part $\overline{p_v}$ in gas mixture $\overline{p}_{v,0} \equiv p_{g,\infty,0}/p_{g,0}$, as well as sprayed liquid yield G_l and gas yield G_g ratio $\overline{g} \equiv G_{l,0}/G_{g,0}$. Parameter $\overline{g_0}$ defines droplet heat and mass transfer and phase transformation impact for carrying gas flow state. In this study, it is stated that a slight amount of water is sprayed into the gas flow: therefore, $\overline{g}_0 \cong 0$ and droplets transfer and phase transformation processes do not have an influence for the gas parameters: $T_g(\tau) \equiv T_{g,0}$ and $p_g(\tau) \equiv p_{g,0}$.

2.1 A model of heat flows balance on the droplet surface

An imagine of droplet that is sprayed in liquid phase transformation cycle $\tau \equiv 0 \div \tau_f$ at a different modelled transfer processes in phase transformation regimes allows to view at them from uniform positions, while forming overall *droplet* problem that is described by expression (1) and forming the *internal* and *external* tasks in this problem. This cycle depends from the sprayed liquid and gas flow parameters.

External task main solutions considered to be external total heat transfer flow $q_{\Sigma}^{+} = q_c^{+} + q_r^{+}$ and liquid vapour flow density on the droplet surface (m_v^{+}). Phase transformation heat flow $q_f^{+} = m_v^{+}L$ is expressed by product of liquid latent heat of evaporation (L)

and m_v^+. *Internal* task main solutions are droplet internal heat transfer total flow $q_\Sigma^- = q_c^- + q_r^-$ and droplet unsteady temperature field $T(r,\tau)$. They are applied to concretize expression (1) according to methodology that was discussed in [8] literature:

$$\frac{\lambda_{vg}(\tau)\mathrm{Nu}(\tau)}{2R(\tau)} \ln \frac{1+B_T(\tau)}{B_T(\tau)} \left[T_g(\tau) - T_R(\tau)\right]$$
$$- \lambda_l(\tau)\,\mathrm{grad}\,T(r,\tau)|_{r=R^-} - L(\tau)\frac{D_{vg}(\tau)\mu_v}{T_R(\tau)R_\mu R(\tau)}$$
$$\times \left[p_{v,R}(\tau) - p_{v,\infty} + \frac{\mu}{\mu_g}\left(p\ln\frac{p-p_{v,\infty}}{p-p_{v,R}}\right) - p_{v,R}(\tau) + p_{v,\infty}\right] = 0. \qquad (2)$$

In expression (2), it is provided that droplet is heated by conduction $\mathrm{Nu} = 2$, while Stefan hydrodynamic flow impact for heating intensity is evaluated by Spalding heat transfer parameter B_T; radiation flow density on the droplet surface both sides is equally $q_r^- \equiv q_r^+$; liquid does not circulate in droplet, therefore, convective heat spread in them is defined according to Fourier thermal conductivity low; thermal conductivity coefficient λ, as well for vapour and gas mixture λ_{vg}, diffusivity coefficient D_{vg} and mass specific heat $c_{p,vg}$ are selected according to temperature $T_{vg} = T_R + (T_g - T_R)/3$; μ_v and μ_g is vapour and gas molecular mass, respectively; R_μ is universal gas constant.

Spalding heat transfer parameter is defined according to recommendations [11] in droplet condensing (*co*) and evaporation (*ee*) phase transformation regimes:

$$B_T = \frac{c_{p,vg}(T_g - T_R)}{L}\frac{q_f^+}{q_k^+}$$

when

$$q_{f\equiv co}^+ = -q_k^+ - \lambda_L k_c^- \left.\frac{\partial T_r}{\partial r}\right|_{r=R^-}, \qquad q_{f\equiv ee}^+ = q_k^+ - \lambda_L k_c^- \left.\frac{\partial T_r}{\partial r}\right|_{r=R^-}. \qquad (3)$$

In expression (3), heat spread in droplet by convection is considered by effective conductivity parameter k_c^-.

Heat flows balance condition (2), that characterizes flows in and from the droplet surface, is closely related with droplet unsteady temperature field function $T(r,\tau)$ that defines droplet thermal parameters $P_T(\tau) \equiv T_R(\tau) = T(r = R^-, \tau)$ and $P_T(\tau) \equiv \mathrm{grad}\,T_{r=R^-}(\tau) = \partial T/\partial r_{r=R^-}$.

It is worth to remember that the droplet center temperature T_C is important to define its non-isothermality $\Delta T(\tau) \equiv T_R(\tau) - T_C(\tau)$, while a droplet mass mean temperature $T_m(\tau) \equiv \int_0^R r^3 \rho_l(r,\tau)T(r,\tau)\,\mathrm{d}r / \int_0^R r^3 \rho_l(r,\tau)\,\mathrm{d}r$ defines its thermal state of non-isothermal droplet.

Thermal parameters have a significant effect for the droplets energy and phase transition parameters. Therefore, the optimal droplet radial coordinate r and time coordinate τ grid is based on the analysis of thermal parameter functions $P_T \equiv T_r(\tau)$ and $P_T \equiv \mathrm{grad}\,T_r(\tau)$.

2.2   By conduction and radiation heated droplet thermal parameters model

In radiant gas flow without slipping drifted semi-transparent droplets, thermal parameters defining functions $P_T(\tau)$ in expression (2) can be described by the infinite series based integral-type model [6]:

$$
P_T(r,\tau) = P_{T,R}(\tau) + \sum_{n=1}^{\infty} F(n,r)
$$

$$
\int_0^{\tau} \left[(-1)^n \frac{R}{n\pi} \frac{\mathrm{d}T_R}{\mathrm{d}\tau} - \frac{1}{R\rho_l c_{p,l}} \int_0^R q_r \left(\sin\frac{n\pi r_*}{R} - \frac{n\pi r_*}{R}\cos\frac{n\pi r_*}{R} \right) \mathrm{d}r_* \right]
$$

$$
\times \exp\left[-a_l \left(\frac{n\pi}{R} \right)^2 (\tau - \tau_*) \right] \mathrm{d}\tau. \tag{4}
$$

In (4), expression ρ_l, $c_{p,l}$ and a_l are liquid density, mass specific heat, and thermal coefficient, respectively. For various thermal parameters, in both $P_{T,R}$ and $F(n,r)$ functions, a different meaning is being provided in expression (4):

$$
P_{T,R}(\tau) \equiv T_R(\tau) \quad \text{and} \quad F(n,r) \equiv \frac{2}{r}\sin\frac{n\pi r}{R} \tag{5}
$$

when $P_T(r,\tau) \equiv T(r,\tau)$;

$$
P_{T,R}(\tau) \equiv T_R(\tau) \quad \text{and} \quad F(n,r) \equiv \frac{2n\pi}{R} \tag{6}
$$

when $P_T(r,\tau) \equiv T(r=0,\tau) = T_C(\tau)$;

$$
P_{T,R}(\tau) \equiv 0 \quad \text{and} \quad F(n,r) \equiv 2\frac{n\pi}{rR}\cos\frac{n\pi r}{R} - \frac{2}{r^2}\sin\frac{n\pi r}{R} \tag{7}
$$

when $P_T(r,\tau) \equiv \operatorname{grad} T_r(\tau) = \partial T(r,\tau)/\partial r$;

$$
P_{T,R}(\tau) \equiv 0 \quad \text{and} \quad F(n,r) \equiv (-1)^n \frac{2\pi n}{R^2} \tag{8}
$$

when $P_T(r,\tau) \equiv \operatorname{grad} T(r=R,\tau) = \partial T(r,\tau)/\partial r|_{r=R}$;

$$
P_{T,R}(\tau) \equiv 0 \quad \text{and} \quad F(n,r) \equiv 0 \tag{9}
$$

when $P_T(r,\tau) \equiv \operatorname{grad} T(r=0,\tau) = \partial T(r,\tau)/\partial r|_{r=0}$.

In phase transformation cycle, a droplet diameter varies: grows in condensing regime, while reduces in evaporation regime. Therefore, the graphical analysis of thermal parameters functions $P_T(r,\tau)$ is very uncomfortable. For system (2)–(9), it is easy to form the numerical research scheme when giving universal form of non-dimensional coordinate for time τ and droplet radial coordinates r. In phase transformations, the coordinate $\eta = r/R(\tau)$ can serve as the non-changing universal droplet radial coordinate (where

$\eta = 0$ – droplet center, $\eta = 1$ – droplet surface). The droplet phase transformation cycle $\tau \equiv 0 \div \tau_f$ is modelled. It is modified with the help of Fourier criteria $\mathrm{Fo} = \tau \cdot a_0 / R_0^2$ and is transformed to a Fourier time scale: $\mathrm{Fo} \equiv 0 \div \mathrm{Fo}_f$.

Fourier time scale is practical because it ensures insensitive thermal parameters functions $P_{T,k}(\mathrm{Fo})$ graphs for droplets dispersity when droplet is heated by conduction (k heating transfer case) [7].

The general expression of thermal parameters (4) in universal coordinates Fo and η will get the following form:

$$
P_T(\eta, \mathrm{Fo}) = P_{T,\eta=1}(\mathrm{Fo}) + \sum_{n=1}^{\infty} F(n, \eta) \frac{R_0^2}{a_{et}}
$$

$$
\times \int_0^{\mathrm{Fo}} \left[(-1)^n \frac{a_{et}}{n\pi} \frac{R}{R_0^2} \frac{\mathrm{d}T_R}{\mathrm{d}Fo} - \frac{1}{p_l c_{p,l}} \int_0^1 q_r(\eta)(\sin n\pi\eta - n\pi\eta\cos n\pi\eta)\,\mathrm{d}\eta \right]
$$

$$
\times \exp\left[-(n\pi)^2 \frac{a_l}{a_{et}} \frac{R_0^2}{R^2} (\mathrm{Fo} - \mathrm{Fo}_*) \right] \mathrm{d}Fo_*. \tag{10}
$$

Here:

$$
P_{T,\eta=1}(\mathrm{Fo}) \equiv T_{\eta=1}(\mathrm{Fo}) \quad \text{and} \quad F(n, \eta) \equiv \frac{2}{\eta R(\mathrm{Fo})} \sin n\pi\eta \tag{11}
$$

when $P_T(\eta, \mathrm{Fo}) \equiv T(\eta, \mathrm{Fo})$;

$$
P_{T,\eta=1}(\mathrm{Fo}) \equiv T_{\eta=1}(\mathrm{Fo}) \quad \text{and} \quad F(n, \eta) \equiv \frac{2n\pi}{R(\mathrm{Fo})} \tag{12}
$$

when $P_T(\eta, \mathrm{Fo}) \equiv T(\eta = 0, \mathrm{Fo}) = T_C(\mathrm{Fo})$;

$$
P_{T,\eta=1}(\mathrm{Fo}) \equiv 0 \quad \text{and} \quad F(n, \eta) \equiv 2\frac{n\pi}{\eta R^2(\mathrm{Fo})} \cos n\pi\eta - \frac{2}{\eta^2 R^2(\mathrm{Fo})} \sin n\pi\eta \tag{13}
$$

when $P_T(\eta, \mathrm{Fo}) \equiv \mathrm{grad}\, T_\eta(\mathrm{Fo}) = (1/R(\mathrm{Fo}))\partial T(\eta, \mathrm{Fo})/\partial\eta$;

$$
P_{T,\eta=1}(\mathrm{Fo}) \equiv 0 \quad \text{and} \quad F(n, \eta) \equiv (-1)^n \frac{2\pi n}{R^2(\mathrm{Fo})} \tag{14}
$$

when $P_T(\eta, \mathrm{Fo}) \equiv \mathrm{grad}\, T(\eta = 1, \mathrm{Fo}) = (1/R(\mathrm{Fo}))\partial T(\eta, \mathrm{Fo})/\partial\eta|_{\eta=1}$;

$$
P_{T,\eta=1}(\mathrm{Fo}) \equiv 0 \quad \text{and} \quad F(n, \eta) \equiv 0 \tag{15}
$$

when $P_T(\eta, \mathrm{Fo}) \equiv \mathrm{grad}\, T(\eta = 0, \mathrm{Fo}) = \partial T(\eta, \mathrm{Fo})/(R(\mathrm{Fo})\partial\eta)|_{\eta=1} = 0$.

Numerical algorithm model of thermal parameters is created according to [7] recommendations.

3 The numerical scheme of droplet thermal parameters

For numerical scheme grid formation, universal radial $\eta = r/R(\tau) \equiv 0 \div 1$ and time $\overline{\mathrm{Fo}} \equiv 0 \div 1$ coordinates are applied, respectively. For phase transformation cycle, an universal unitary duration is formed by normed Fourier criterion Fo. Fourier criteria is normed in aspect of freely chosen $\mathrm{Fo}_f \colon 0 \div \tau_f \to 0 \div \mathrm{Fo}_f \to 0 \div \mathrm{Fo}/\mathrm{Fo}_f \equiv 0 \div 1$. In phase transformation cycle, the droplets unitary dimension is divided in $J - 1$ parts. Universal unitary duration of phase transformation cycle is divided into $I - 1$ parts. Defining radial η and Fourier criteria $\mathrm{Fo}_i = \overline{\mathrm{Fo}}_i \cdot \mathrm{Fo}_f$ coordinates, the follwing conditions are ensured:

$$\sum_{j=2}^{J}(\eta_j - \eta_{j-1}) = 1 \quad \text{and} \quad \sum_{i=2}^{I}(\overline{\mathrm{Fo}}_j - \overline{\mathrm{Fo}}_{j-1}) = 1. \tag{16}$$

In the infinite sum of expression (10), the assessed member of number N is defined, and its integrals are changed by finite sums:

$$P_{T,i,j} = P_{T,i,J} + \frac{R_0^2}{a_{et}}\sum_{n=1}^{N}F_{i,j,n}\sum_{ii=2}^{1<i\leqslant I}\left[(-1)^n\frac{a_{et}}{n\pi}\frac{R_{ii-1}}{R_0^2}\frac{T_{ii,J}-T_{ii-1,J}}{\mathrm{Fo}_{ii}-\mathrm{Fo}_{ii-1}}\right.$$

$$\left. -\frac{1}{\overline{\rho}_{l,ii,j}\overline{c}_{p,l,ii,j}}\sum_{jj=2}^{J}\overline{q}_{r,ii,jj}\int_{\eta_{jj-1}}^{\eta_{jj}}(\sin n\pi\eta_* - n\pi\eta_*\cos n\pi\eta_*)\,\mathrm{d}\eta_*\right]$$

$$\times\int_{\mathrm{Fo}_{ii-1}}^{\mathrm{Fo}_{ii}}\exp\left[-(n\pi)^2\frac{a_l(\mathrm{Fo})}{a_{et}}\frac{R_0^2}{R^2(\mathrm{Fo})}(\mathrm{Fo}-\mathrm{Fo}_{ii})\right]\mathrm{dFo}. \tag{17}$$

In expression (17), $\overline{\rho}_{l,ii,j} \equiv (\rho_{l,ii,j} + \rho_{l,ii-1,j})/2$, $\overline{c}_{pl,ii,j} \equiv (c_{pl,ii,j} + c_{pl,ii-1,j})/2$, $\overline{q}_{r,ii,j} \equiv (q_{r,ii,j} + q_{r,ii,j-1})/2$. Expressions (11)–(15) are applied to calculate parameters $P_{T,i,J}$. In expression (17), integrals are solved analytically, and a numerical scheme is created to calculate the droplets thermal parameters:

$$P_{T,i,j} = P_{T,i,J} + \frac{R_0^2}{a_{et}}\sum_{n=1}^{N}F_{i,j,n}\sum_{ii=2}^{1<i\leqslant I}\left[(-1)^n\frac{a_{et}}{n\pi}\frac{R_{ii-1}}{R_0^2}\frac{T_{ii,J}-T_{ii-1,J}}{\mathrm{Fo}_{ii}-\mathrm{Fo}_{ii-1}}\right.$$

$$\left. +\frac{f_{1,n}}{\overline{\rho}_{l,ii,j}\overline{c}_{p,l,ii,j}}\right]\frac{2}{n^2\pi^2}\frac{a_{et}}{a_{l,ii}+a_{l,ii-1}}\frac{R_{ii-1}^2}{R_0^2}f_{2,n}.$$

Here

$$f_{1,n} = \sum_{jj=2}^{J}\overline{q}_{r,ii,jj}\left(\eta_{jj}\sin n\pi\eta_{jj} + \frac{2}{n\pi}\cos n\pi\eta_{jj}\right.$$

$$\left. -\eta_{jj-1}\sin n\pi\eta_{jj-1} - \frac{2}{n\pi}\cos n\pi\eta_{jj-1}\right),$$

$$f_{2,n} = \exp\left[n^2\pi^2 \frac{a_{l,ii} + a_{l,ii-1}}{2a_{et}} \frac{R_0^2}{R_{ii-1}^2}(\mathrm{Fo}_{ii} - \mathrm{Fo}_i)\right]$$
$$- \exp\left[n^2\pi^2 \frac{a_{l,ii} + a_{l,ii-1}}{2a_{et}} \frac{R_0^2}{R_{ii-1}^2}(\mathrm{Fo}_{ii-1} - \mathrm{Fo}_i)\right]. \tag{18}$$

After providing the values of parameters J and I, the numerical scheme grid is graded in aspect to the universal radial and the time coordinate that is expressed by Fourier criterion. In the infinite sum, the optimal number of assessed member is accepted $N_{op} = 121$ [8]. Starting with $i = 2$, for each $\mathrm{Fo}_{i \geqslant 1}$, an iterative cycle is carried out in order to define temperature $T_{J,i}$, which satisfies the droplet surface energy flow balance condition (2) in parallel calculated droplet thermal parameters $P_{T,i}$ according to expression (3). At the end of each iterative cycle, according to discussed methodology in [2], the variation of droplet dimension is defined as $\Delta R_i = R_i - R_{i-1}$. In the case of compound heating by conduction and radiation ($k + r$ heat transfer), the local radiation flow in the droplet is calculated by the methodology of [6] providing the existence of absolute black gas temperature outer radiation source.

The discussed numerical scheme can be applied for modelling separate regimes of water droplet phase transformation cycle. Then an universal duration cycle $\overline{\mathrm{Fo}} \equiv 0 \div 1$ is formed when Fourier number is selected as the main normalizing criteria Fo_f that defines the modelled phase transformation duration etc. For condensing phase transformation regime, this is $\mathrm{Fo}_f \equiv \mathrm{Fo}_{co}$.

4 Optimal grading of time and droplet radial coordinates

The numerical iterative scheme functionality and results reliability of the droplet phase transformations numerical modelling depends from an appropriate selection of the parameters J and I. It is practically impossible to predict the optimal values of these parameters because of the nonlinearity of compound heat and mass transfer processes in the semitransparent droplet and in gas two-phase flow. The optimal parameters J_{op} and I_{op} of numerical scheme grid can only be defined by scrupulous numerical experiment. The numerical scheme grid defining parameters are affected by the droplet heating method and boundary condition that defines liquid spray, as well as gas flow, parameters.

The optimal grading of the radial coordinate should ensure a detailed evaluation of compound heat transfer process interaction within the droplet. In this interaction, factors of the heat radiation absorption at semitransparent liquid [6] and phase transformation regime variation [11], are important. Providing that radiation factor is essential for heat spread in droplet, the radial coordinate optimal grading is expressed by radiation and conduction for the droplet heated at the air. Sprayed water droplet was modelled at 290 K temperature, hat has a diameter of 150 micrometres. Its phase transformation cycle was simulated in dry air at 1000 K degrees. In comparable analysis, the numerical scheme grid of parameters ($N = 121$, $J = 61$, $I = 81$, $M = 81$) considered to be the basic. Based on the peculiarities of heat radiation and thermal conduction process interaction, defined
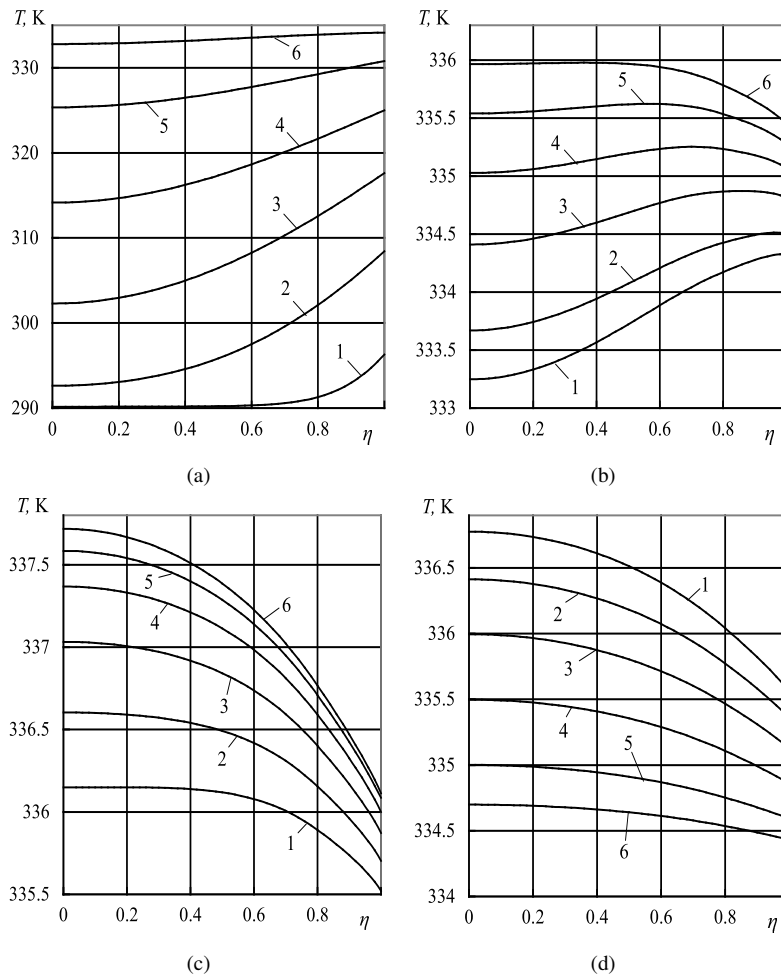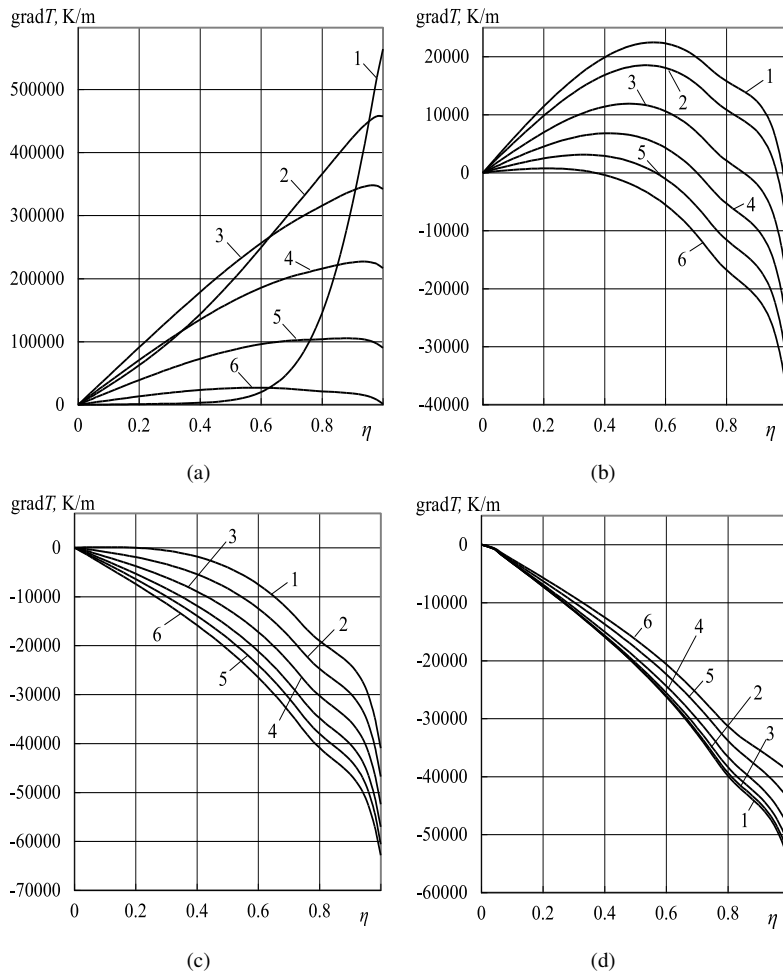
Figure 1. The unsteady temperature field at the water droplet in its primary (a), transit (b), and at final unsteady evaporation (c), as well in equilibrium evaporation (d) regimes in case of compound droplet heating by radiation and conduction. (a) Fo = 0.0175, 0.0875, 0.175, 0.28, 0.42, 0.595, (b) Fo = 0.6125, 0.63, 0.665, 0.7, 0.735, 0.77, (c) Fo = 0.7875, 0.84, 0.91, 0.9975, 1.1025, 1.335, (d) Fo = 3.625, 4.25, 4.875, 5.5, 6, 6.25 (resp. curves 1–6); $T_g = 1000$ K, $p = 0.1$ MPa, $\overline{p} = 0$, $T_0 = 290$ K, $T_{sr} \equiv T_g$.

in non-stationary temperature field within the water droplet, the primary, transitional, and final droplet thermal state change periods have been separated (Fig. 1). The distribution of temperature inside the droplet defines regularities of temperature field local gradient (Fig. 2), They leads to redistribution peculiarities of thermal energy inside the droplet.

In the primary period, the droplet surface outer layers of the droplet heat up more intensively the maximum value of function $T(\eta, \text{Fo})$ is on the surface of the droplet (Fig. 1(a)): $T(\eta = 1, \text{Fo}) \equiv T_{\max}(\text{Fo}) \equiv T_R(\text{Fo})T(\eta, \text{Fo})$. In this period, the radiation flow, which is absorbed in the droplet accelerates the heating of its central layers,

Figure 2. The unsteady temperature field gradient at the water droplet in its primary (a), transit (b), and final transit evaporation (c), as well in equilibrium evaporation (d) regimes in case of compound droplet heating by radiation and conduction. $\operatorname{grad} T \equiv \partial T(\eta, \mathrm{Fo})/\partial \eta$, K/m. Everything else is the same as in Fig. 1.

however, the temperature field gradient remains positive (Fig. 2(a)). An interaction of compound transfer processes in the droplet at transit thermal state change period is very intensive and causes unsteady temperature deformations in the central droplet layers (Fig. 1(b)). These deformations characterizes the essential changes of temperature field local gradients (Fig. 2(b)). During the transit droplet thermal state change period, the maximum temperature from droplet surface consistently passes to its center. Due to observed peculiarities of temperature local gradient in the droplet (Fig. 2(b)), absorbed thermal energy of radiation is redistributed in two directions by thermal conduction: in the surface layers – towards the surface of the droplet (the temperature field gradient is negative in them), and in central layers – towards the centre of the droplet (the temperature field gradient is
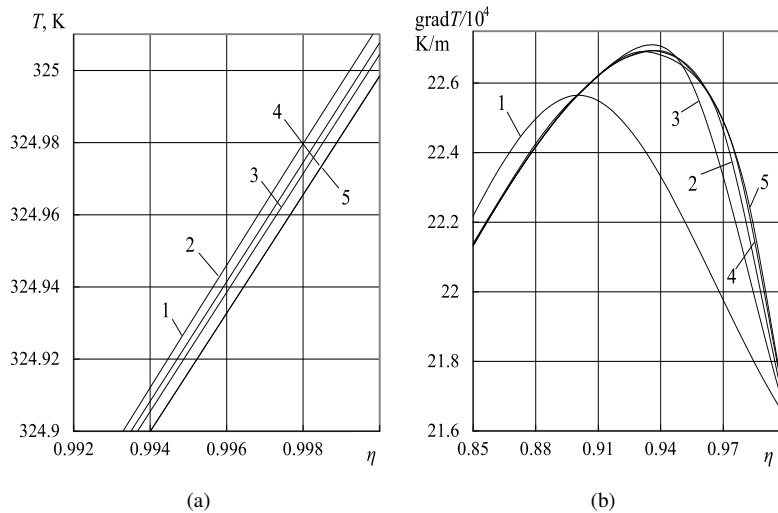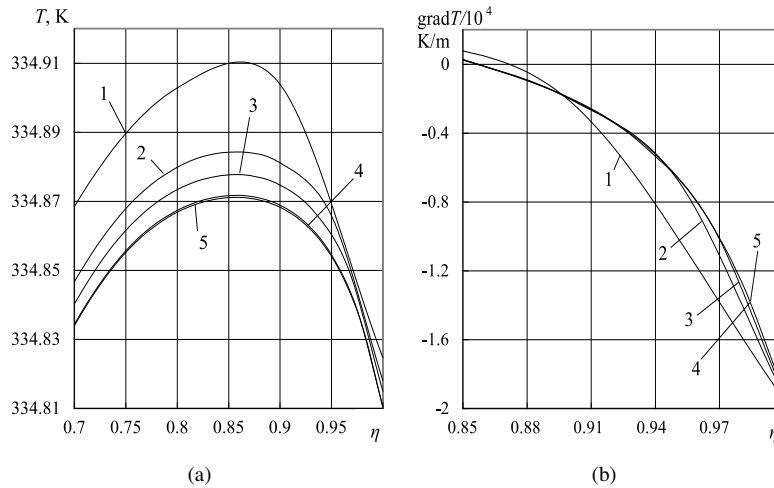
Figure 3. The droplets radial coordinate grading influence for temperature field in the droplet (a) and for its gradient (b) in the droplets thermal state change initial period when Fo = 0.28, T_g = 1000 K $p = 0,1$ MPa, $\bar{p} = 0$, $T_0 = 290$ K, $T_{sr} \equiv T_g$, $J = 11, 21, 31, 41, 61$ (resp. curves 1–5).

still positive). The final droplet thermal state change period begins when the maximum temperature of the unsteady field reaches the center of the droplet. Regimes of transit (Fig. 1(c)) and equilibrium (Fig. 1(d)) evaporations can be distinguished. At the beginning of transit regime, the droplet still heats up. In whole droplet, the formulated negative temperature field gradient creates preconditions for thermal energy that is absorbed by radiation to output it to droplet surface by conduction. This part of radiation flow already has been involved in liquid evaporation process. At the end of transit evaporation regime, the droplet heats up maximally (Fig. 1(c), 6th curve). From this moment the whole thermal energy is provided for the droplet starts to participate in water evaporation process, therefore, $q_f^+ = q_c^+ + q_r$ because $q_k^+ = q_r$. At equilibrium evaporation regime, the droplet cools down (Fig. 1(d)). The droplet cooling is caused by reduced radiation absorption in decreasing droplet [6]. The negative gradient temperature field remains (Fig. 2(d)).

When defining the parameter J_{op}, the radial coordinate was gridded linearly: $\eta = (j-1)/(J-1)$ when $j = 1, J$. The parameter J was changed from 11 to 61. The dividing number J influence for calculated P_T parameters is evaluated at initial and transit droplet thermal state change periods, where droplet hats up more intensively, here Fo $\equiv 0.28$ (Fig. 3) and Fo $\equiv 0.84$ (Fig. 4), respectively. It is clear that $J > 41$ is not worth taken. Therefore, the case of $J_{op} = 41$ is accepted as the optimal droplet radial coordinate grid.

The optimal time coordinates grading should guarantee an equivalent attention to the transfer process interaction in whole droplet phase transformation regime cycle. The duration of phase transformation regimes can be distinctly different in both real and Fourier criteria time scales. Therefore, during the numerical experiment, this ought to be taken into account. Here, for each phase transformation regime, an universal duration $0 \div 1$ is provided that it is essentially based on the time coordinate $\overline{\text{Fo}}$ [7]. Then phase

Figure 4. The droplet radial coordinate grading influence for the temperature field in the droplet (a) and for its gradient (b) at the droplet thermal state change initial period when $\mathrm{Fo} = 0.84$, $T_g = 1000$ K, $p = 0.1$ MPa, $\overline{p} = 0$, $T_0 = 290$ K, $T_{sr} \equiv T_g$.

transformation cycle $0 \div \mathrm{Fo}_{co} \div \mathrm{Fo}_{uf} \div \mathrm{Fo}_{ee}$ is transformed to universal unit duration phase transformation regime cycle $0 \div 1 \div 2 \div 3$. Here $0 \div 1$ – condensation regime, $1 \div 2$ – transit evaporation regime, $2 \div 3$ – equilibrium evaporation regime. In these regimes, as the normed factor, the duration of corresponding period is being used: Fo_{co}, Fo_{uf} or Fo_{ee} [7].

The aspect of condensation phase transformation regime change to transit evaporation regime is very important. It is related with peculiarities of vapour flow function $g_v(\mathrm{Fo})$. The change of phase transformation regime from condensation to evaporation occur when droplet surface heats up to the dew point temperature. At this moment vapour flow on the droplet surface when moving zero value $g_v(\mathrm{Fo} \equiv \mathrm{Fo}_{co}) = 0$, changes the flow direction: in condensation regime flows toward the droplet while in evaporation regime spread from its. At the time moment $\mathrm{Fo}_i \cong \mathrm{Fo}_{co}$ the sub-program, which performs the iterative calculation of droplet surface temperature $T_R(\mathrm{Fo} \cong \mathrm{Fo}_{co})$ by fastest descent method, cannot ensure the fulfillment of the requirement $\mathrm{error} < 0.025$ raised for equation (1) solution (Fig. 5(a)). This have influenced calculated functions $T_R(\mathrm{Fo})$ and $g_0(\mathrm{Fo})$ that is important for the droplet heat transfer and phase transformations (Fig. 5(b)). To prevent this, the numerical experiment is carried out into three stages. In each of them, constant parameters of numerical scheme is kept $N_{op} = 121$, $J_{op} = 31$, and $M = 81$. Here size M evaluates the dividing number of radiation spectrum. The time grid grading parameter I is chosen individually.

When $T_{dp}/T_0 > 1$, the first phase transformation cycle regime is condensation. It is modelled independently. The time grid in the numerical scheme is graded in aspect of the condensation regime universal unitary time duration providing the control Fo_i time moment number $I \equiv I_{co}$: $\Delta \overline{\mathrm{Fo}}_i = 1/(I_{co} - 1)$. Then the modelled phase transition regime $0 \div \mathrm{Fo}_{co,sp}$ and time step $\mathrm{Fo}_i = \Delta \mathrm{Fo}_i \cdot \mathrm{Fo}_{co,sp}$ are defined by the guessed Fourier
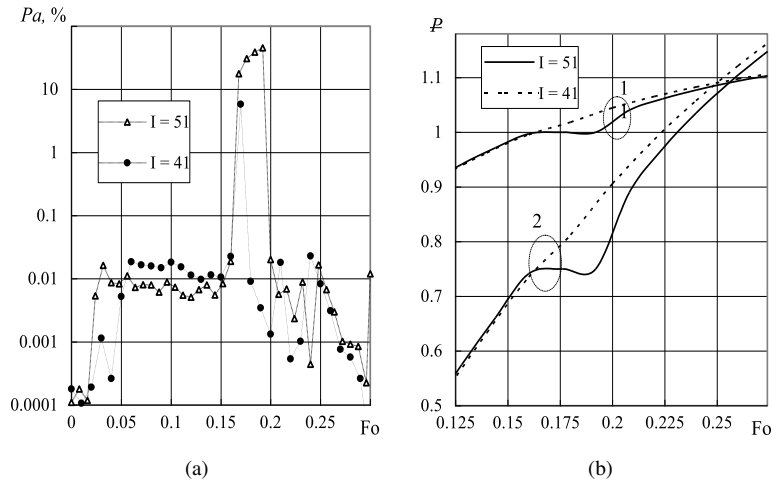
Figure 5. The iterative scheme instability impact for heat flows imbalance on the droplet surface when phase transformations nature variates (a) and for calculated functions $\overline{T}_R \equiv (T_R - 273.15)/(T_{dp} - 273.15)$ and $\overline{m} \equiv m_v/|m_{v,0}|$ in k heat transfer case; $\overline{P} \equiv \overline{T}_R$, $\overline{P} \equiv \overline{m}_v + 0,75$ (resp. curves 1–2).

criterion $\mathrm{Fo}_{co,sp}$. It is guessed that the condensation regime will end within time step of 61 divisions. For this case, the modelled condensation phase transformation regime $0 \div \mathrm{Fo}_{co}$ is considered as supporting. It is reached that the temperature of droplets surface in the end of the condensation regime would possibly better meet the droplet dew point temperature, but would not exceed it. By numerical experiment it is defined that $\mathrm{Fo}_{co} = 0.1583$ in k heat transfer case. The reached result is $T_{R,I_{co}\equiv 61} = 338.141$ when $T_{dp} = 338.1532$. Then $R_{I_{co}} = 75.853 \cdot 10^{-6}$ m, $T_{C,I_{co}} = 310.722$ K, $T_{m,I_{co}} = 328.028$, and $m_{v,I_{co}} = -4 \cdot 10^{-6}$ kg/(m²s).

When grading time coordinate grid, the parameter I has been changed from 11 to 61. The results of the numerical experiment have shown (Fig. 6) that the time grid for the condensation phase transition regime is optimally graded when the division number is chosen in the interval from 30 to 40. For further numerical experiment, choosing $I_{co,op} = 31$, it is adjusted that $\mathrm{Fo}_{co} = 0.161$. The reached result is $T_{R,I_{co}\equiv 31} = 338.1507$ K, $T_{C,I_{co}\equiv 31} = 310,95$ K, $T_{m,I_{co}} = 328.31$ K, $R_{I_{co}\equiv 31} = 75.866 \cdot 10^{-6}$ m, $m_{v,I_{co}} = -4.2 \cdot 10^{-6}$ kg/(m²s).

In the second stage of the numerical experiment, the transit phase transformation regime $0 \div \mathrm{Fo}_{co} \div \mathrm{Fo}_{uf}$ is modelled. For transit regime, a step defined in the first stage $I_{co} = 31$ are kept. Simulation are started again from $\mathrm{Fo}_{i=1} = 0$. Parameter $I_{uf,op}$ for the transit evaporation regime is defined analogously to the condensation regime, however, the research is facilitated by the fact that at the final stage of transit evaporation, the problem of instability of the iterative scheme does not arise because the nature of phase transition does not change when moving to equilibrium evaporation.

Therefore, the droplet surface temperature at the end of transit evaporation regime does not require a strict match of equilibrium evaporation temperature. The transit phase transformation regime duration are defined approximately by $\mathrm{Fo}_{uf} \cong 1.2$, and after
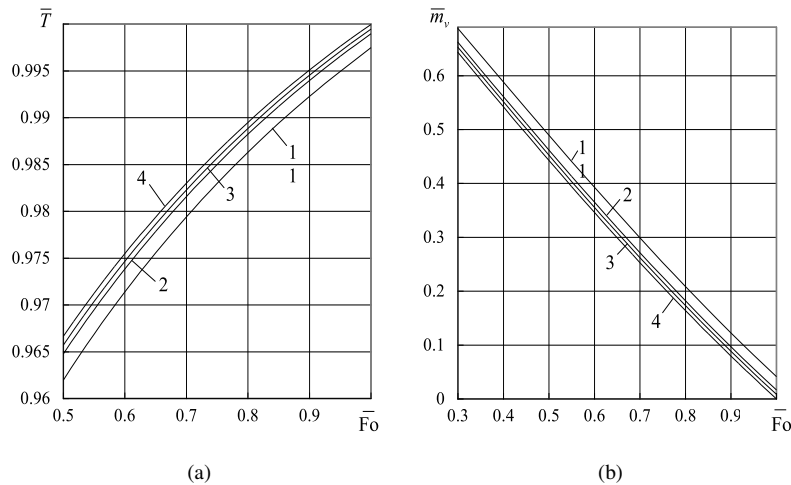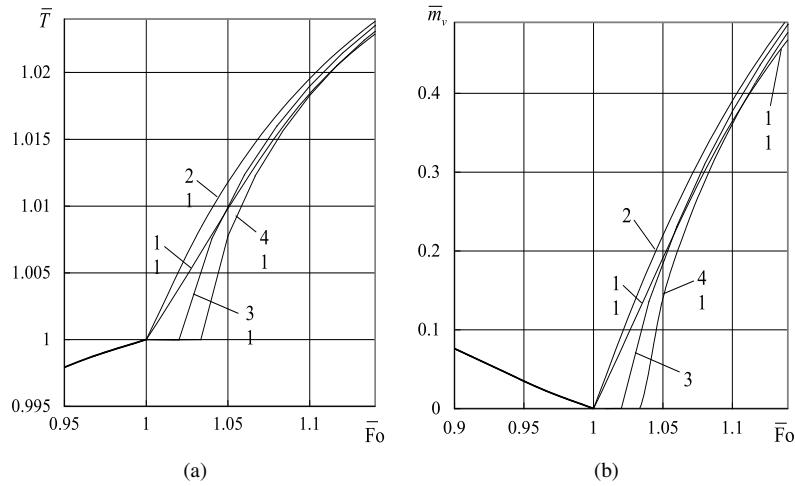
Figure 6. The time coordinate grading in the numerical scheme impact for water droplet thermal (a) and phase transformation (b) parameters in condensing phase transformation regime at the case of k heat transfer. $T_g = 1000$ K, $\overline{p} = 0.25$, $T_0 = 290$ K, $R_0 = 75 \cdot 10^{-6}$ m, $\mathrm{Fo}_{co} = 0.1583$, $I_{co} = 11, 21, 31, 61$ (resp. curves 1–4).

assessing the calculated condensation duration, $\mathrm{Fo}_{uf} \cong 1.039$. For transit evaporation regime, $\Delta\overline{\mathrm{Fo}}_i = 1/I_{uf}$. Parameter I_{uf} was consistently increased from 10 to 60 by step 10.

Displaying the consistent modeling results of the phase transformations, a unique time coordinate is applied. For the condensing phase transformation regime $0 \div 1$, its universal unitary time duration is normed according to $\overline{\mathrm{Fo}}_{0\div1} \equiv \mathrm{Fo}/\mathrm{Fo}_{co}$, while for the transit evaporation $1 \div 2$ regime, its unitary time duration is $\overline{\mathrm{Fo}}_{0\div2} \equiv 1 + (\mathrm{Fo}_{uf} - \mathrm{Fo}_{co})/\mathrm{Fo}_{uf}$. It is clear that an overly small time grid grading can cause instability of the numerical scheme at the initial stage of transit evaporation (Fig. 7, curves 1–3). This is related with the first iterative cycle of transit evaporation regime, where a droplet surface temperature must "skip" a dew point temperature barrier. In the modelled case, the optimal transit evaporation regime time grid is insured by the parameter I_{uf} in the interval $30 \leqslant I_{op} \leqslant 40$. For further numerical experiment, the division number of $I_{uf,op} = 30$ has been chosen.

The full phase transformation regime cycle $0 \div \mathrm{Fo}_{co} \div \mathrm{Fo}_{uf} \div \mathrm{Fo}_f$ is modelled in the third stage of the numerical experiment. The duration $\mathrm{Fo}_f \approx 7$ of this cycle must be guessed at the beginning. Then the equilibrium evaporation duration is $\mathrm{Fo}_{ee} \approx 5.8$.

The numerical scheme grid previously defined by parameters $I_{co} = 31$ and $I_{uf} = 30$ is maintained for transit phase transformation $0 \div \mathrm{Fo}_{co} \div \mathrm{Fo}_{uf}$ regime. For equilibrium evaporation regime, the time grid is graded in aspect to its universal unary length of time: $\Delta\overline{\mathrm{Fo}}_i = 1/I_{ee}$. The equilibrium regime ends when the droplet is fully evaporated, therefore equilibrium evaporation duration is defined according to graphs of functions of phase transformation. During numerical research, parameter I_{ee} is increased from 10 by 10 until an acceptable parameter $I_{ee,op}$ value interval $60 \leqslant I_{eg,op} \leqslant 70$ (Fig. 8) is

Figure 7. The time coordinate grading impact for water droplet surface temperature function $\overline{T} \equiv T_R/T_{dp}$ (a) and vapour density flow function $\overline{m}_v \equiv m_v/m_{v,0}$ (b) at transit evaporation in the numerical scheme. $T_g = 1000$ K, $\overline{p} = 0.25$, $T_0 = 290$ K, $R_0 = 75 \cdot 10^{-6}$ m, $m_{v,0} = 0.1706$ kg/(m^{2}s), Fo$_{co} = 0.161$, $I_{co} = 31$, Fo$_{uf} = 1.2$, $T_{e,k} = 349.998$ K, $I_{uf} = 10, 30, 50, 60$ (resp. curves 1–4).
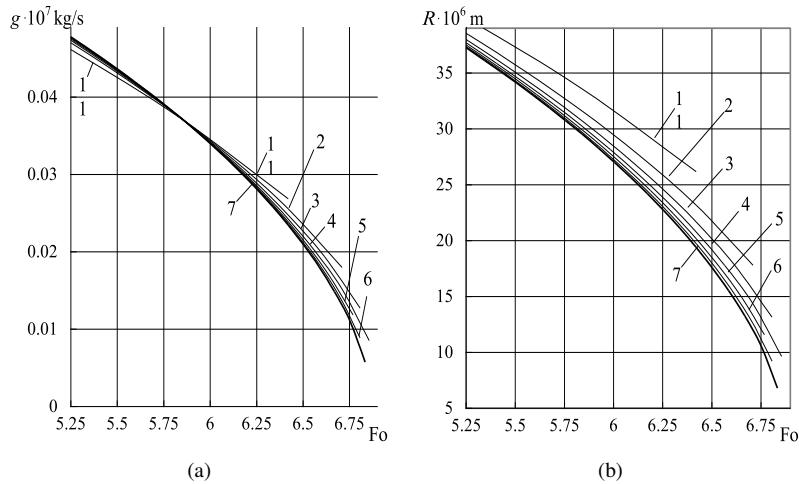
Figure 8. The impact of parameter I_{ee} for the calculated functions $R(\mathrm{Fo})$ and $g_v(\mathrm{Fo})$ in the droplet equilibrium evaporation regime in the k heat transfer case when $T_g = 1000$ K, $\overline{p} = 0.25$, $T_0 = 290$ K, $R_0 = 75 \cdot 10^{-6}$ m, Fo$_{co} = 0.161$, $I_{co} = 31$, Fo$_{uf} = 1.2$, $I_{uf} = 31$, Fo$_{ee} = 5.8$, $I_{ee} = 10, 20, 30, 40, 50, 60, 70$ (resp. curves 1–7).

defined by the calculated functions $R(\mathrm{Fo})$ change trend. Assuming that $I_{ee,op} \equiv 60$, the equilibrium evaporation regime duration is specified: Fo$_{ee} \approx 5.7$.

For the full phase transformation cycle $0 \div 1 \div 2 \div 3$, a graphical interpretation of the calculated functions $P_k(\mathrm{Fo})$ is provided for the condensation $0 \div 1$ and $1 \div 2$ transit
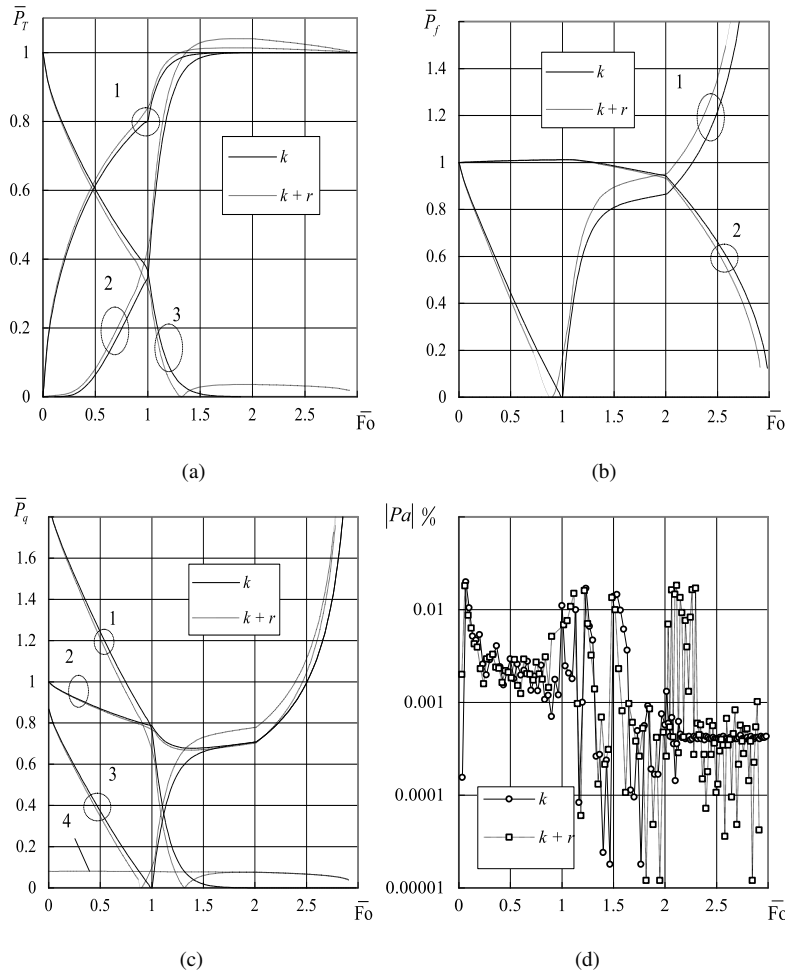
Figure 9. The variation of water droplet: thermal (a), phase transformations (b) and energy (c) parameters, as well energy flow imbalance (d) in the cases of k and $k + r$ heat transfer cases. $T_{sr} \equiv T_v$, $T_g = 1000$ K, $\overline{p} = 0.25$, $T_0 = 290$ K, $R_0 = 75 \cdot 10^{-6}$ m, $\mathrm{Fo}_{co,k} = 0.161$, $\mathrm{Fo}_{co,k+r} = 0.145$, $\mathrm{Fo}_{uf,k} = 1,039$, $\mathrm{Fo}_{ee,k} = 5.7$, $I_{co} = 31$, $I_{uf} = 30$, $I_{ee} = 60$, $q_{k,0}^+ = 483.43$ kW/m², $q_{k,0}^+ = 419.83$ kW/m²; $\overline{T} \equiv (T - T_0)/(T_{e,k} - T_0)$; $\mathrm{grad}\,T_R(0) = 1527227$ K/m; $\partial \overline{T}/\partial r \equiv \mathrm{grad}\,T_R(\mathrm{Fo})/\mathrm{grad}\,T_R(\mathrm{Fo} = 0)$, $\overline{P}_q \equiv P_q/q_k^+$. (a) $\overline{T}_R$, $\overline{T}_C$, $\partial \overline{T}_R/\partial r$ (rep. curves 1–3); (b) $\overline{m}_v$, $\overline{R}$ (rep. curves 1–2); (c) $\overline{q}_k^-$, $\overline{q}_k^+$, $\overline{q}_f^+$, $\overline{q}_r^-$ (rep. curves 1–4).

evaporation regimes, while maintaining the before discussed regime length norming, whereas for equilibrium evaporation regime $2 \div 3$ by $\overline{\mathrm{Fo}}_{2 \div 3} \equiv 2 + (\mathrm{Fo}_f - \mathrm{Fo}_{uf})/\mathrm{Fo}_{ee}$.

When modeling the droplet phase transformation cycle in cases of compound heating by conduction and radiation, the numerical scheme grid is kept for defining a k heat transfer case. However, the duration of condensation phase transformation regime that changed due to the effect of radiation must be clarified in order to avoid a possible insta-

bility of the iterative scheme at the end of the first regime. The parameter $\mathrm{Fo}_{co,k} = 1.45$ was defined for $k + r$ heat transfer with an additional numerical research $0 \div 1$ of condensation regime. In the universal phase transformation cycle $0 \div 1 \div 2 \div 3$, while graphically interpreting droplet transfer parameter functions $P_{k+r}(\overline{\mathrm{Fo}})$, the norming parameters are kept in the case of k heat transfer defined $\mathrm{Fo}_{co,k}$, $\mathrm{Fo}_{uf,k}$ and $\mathrm{Fo}_{ee,k}$ (Fig. 9, dashed lines). Then the deviation of functions $P_k(\overline{\mathrm{Fo}})$ graphs from the graphs of functions $P_k(\overline{\mathrm{Fo}})$ are apparently illustrative of the effect that heating conditions more advanced than conduction have on the duration of droplet phase transition mode and carryover parameters within them. The method of droplet heat transfer is significant to all its transfer process parameters. This is confirmed by the change tendencies of distinctive droplet thermal (Fig. 9(a)), phase transformations (Fig. 9(b)), and energetic (Fig. 9(c)) parameter functions $\overline{P}_k(\overline{\mathrm{Fo}}) \equiv P_k(\overline{\mathrm{Fo}})/P_0$ and $\overline{P}_{k+r}(\overline{\mathrm{Fo}}) \equiv P_{k+r}(\overline{\mathrm{Fo}})/P_0$, although normalizing parameters in them are identical.

5 Conclusion

Liquid droplet heat and mass transfer processes are convenient to model numerically by transferring the droplet lifetime $0 \div \tau_f$ to the Fourier time scale and forming unit, which combines condensing, transit, and equilibrium phase transformation regimes duration of universal supporting cycle $0 \div 1 \div 2 \div 3$. In order to form this cycle, the values of Fourier criterion $\mathrm{Fo}_{co,k}$, $\mathrm{Fo}_{uf,k}$ and $\mathrm{Fo}_{ee,k}$, which are defined in the case of k heat transfer, are adapted.

It is appropriate to model sprayed liquid phase transformations by the three-stage numerical experiment methodology, which ensures an adequate approach to each separate phase transformation regime. An optimal grading of the numerical scheme grid is selected for each stage.

The optimized iterative scheme ensures a high balance for calculated heat flows on the surface of the droplet (Fig. 9(d)) while enabling to sparingly use machine computation time, which is relevant in cases of transfer process modelling in sprayed liquid droplet ensembles.

In different cases of droplet heat transfer, for the universal phase transition cycle $0 \div 1 \div 2 \div 3$, it is appropriate to form a graphical interpretation of the transfer parameter functions $\overline{P}(\overline{\mathrm{Fo}})$, which ensures an equivalent transfer process interaction assessment in different condensing, non-stationary evaporation, and equilibrium evaporation regimes.

References

1. N.A. Fuchs, *Evaporation and Droplet Growth in Gaseous Media*, Pergamon Press, London, 1959.

2. C.S. Funk, B. Winzer, W. Perkert, Correlation between shape, evaporation mode and mobility of small water droplets on nanorough fibers, *J. Colloid Interf. Sci.*, **417**:171–179, 2014.

3. D. Ju, J. Xiao, Z. Geng, Z. Huang, Effect of mass fractions on evaporation of a multi-component droplet dimethyl ether (DME)/n-heptane-fueled engine conditions, *Fuel*, **118**:227–237, 2014.

4. K.H. Kim, H.J. Ko, K. Kim, H. Perec-Blanco, Analysis of water droplet evaporation in a gas turbine inlet fogging process, *Appl. Therm. Eng.*, **33-34**:62–69, 2012.

5. T. Kitano, J. Nishio, R. Kurose, S. Komori, Effects of ambient pressure, gas temperature and combustion reaction on droplet evaporation, *Combust. Flame*, **161**:551–564, 2013.

6. G. Miliauskas, Regularities of unsteady radiative-conductive heat transfer in evaporating semitransparent liquid droplets, *Int. J. Heat Mass Transfer*, **44**:785–798, 2001.

7. G. Miliauskas, Universal cycle of the phase transformation regimes for pure liquid droplets. 1. Cycle formation method and numerical modeling framework for droplet transfer processes, *Power Eng.*, **60**(2):77–95, 2014.

8. G. Miliauskas, A. Adomavičius, M. Maziukienė, Modelling of water droplets heat and mass transfer in the course of phase transitions. I: Phase transitions cycle peculiarities and iterative scheme of numerical research control and optimization, *Nonlinear Anal. Model. Control*, **21**(1):135–151, 2016.

9. G. Miliauskas, V. Garmus, The peculiarities of hot liquid droplets heating and evaporation, *Int. J. Heat Mass Transfer*, **52**:3726–3737, 2009.

10. G. Miliauskas, K. Norvaisiene, A systematic evaluation of the unsteady transfer process interaction in evaporating droplets, *Power Eng.*, **59**(1):26–41, 2013.

11. G. Miliauskas, S. Sinkunas, G. Miliauskas, Evaporation and condensing augmentation of water droplets in flue gas, *Int. J. Heat Mass Transfer*, **53**(5–6):1220–1230, 2010.

12. S.S. Sazhin, Advanced models of fuel droplet heating and evaporation, *Prog. Energ. Combust.*, **32**:162–214, 2006.

13. S.S. Sazhin, M. Al Qubeissi, R. Kolodnytska, A.E. Elwardany, R. Nasiri, M.R. Heikal, Modelling of biodiesel fuel droplet heating and evaporation, *Fuel*, **115**:559–572, 2014.

14. S. Shanthanu, S. Raghuram, V. Raghavan, Transient evaporation of moving water droplets in steam–hydrogen–air environment, *Int. J. Heat Mass Transfer*, **64**:536–546, 2013.

15. W.A. Sirignano, *Dynamics and Transport Processes of Sprays*, Cambridge Univ. Press, 1999.

16. J.B. Young, Condensation and evaporation of liquid droplets at arbitrary Knudsen number in the presence of an inert gas, *Int. J. Heat Mass Transfer*, **36**:2941–2956, 1993.

17. Droplet evaporation, 2014, `http://www.sciencedirect.com`.